

## Intramolecular Interactions in Diiodonaphthalenes

Igor Novak\* and Huiming Jiang

Department of Chemistry and CPEC Centre, National University of Singapore, Singapore 117543, Singapore

Branka Kovač

Physical Chemistry Division, "R. Bošković" Institute, HR-10000, Zagreb, Croatia

Received: August 20, 2002

The synthesis and the electronic structure of isomeric diiodonaphthalenes is described. The electronic structure has been investigated by HeI/HeII photoelectron spectroscopy and non-Koopmans' quantum chemical calculations. The influence of the topology of iodine substitution on the electronic structure is discussed. Special emphasis is placed on elucidating the role of intramolecular iodine–iodine interactions.

### Introduction

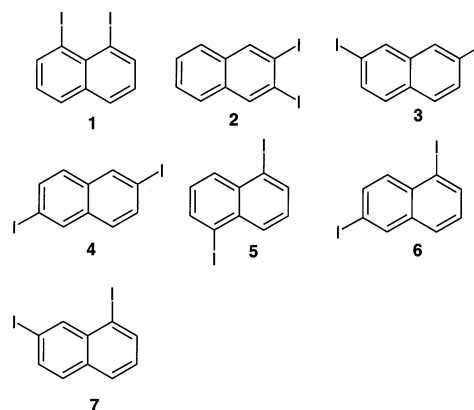
The distortion of molecular structure induced by steric overcrowding or repulsion has been of interest to chemists for a long time. An example of a molecule where such overcrowding takes place is 1,8-diiodonaphthalene. The X-ray diffraction analysis has revealed that the two iodine atoms are twisted out of the rings plane by angles of 5–17° within six crystallographically independent molecules<sup>1</sup>. Despite the twist, iodine–iodine internuclear distances which range from 3.51 to 3.54 Å are still considerably shorter than the sum of iodine van der Waals radii (4.30 Å). It is interesting to compare this structural distortion with the magnitude of repulsive  $\sigma$ -type interactions between 15p orbitals (lone pairs). We have therefore prepared a series of diiodonaphthalenes in order to study such through-space (TS) I–I interactions. UV photoelectron spectroscopy (UPS) allows direct probing of the energy consequences of such interactions and thus complements the results of X-ray study.

The iodine lone pair bands revealed in UPS are sharp and strong and can be readily identified through HeI/HeII measurements. Two types of substituent effects are usually distinguished theoretically: inductive and resonance. This distinction is often difficult to make in the UPS data because both effects "operate" simultaneously. However, the diiodonaphthalenes are isomeric, and hence, the inductive effects can be expected to be of the same magnitude. This permits one to attribute differences in the electronic structures of isomers mainly to resonance effects and thus consider the two effects separately.

### Experimental and Theoretical Methods

**Sample Preparation.** 1,8-diiodonaphthalene (**1**), 2,3-diiodonaphthalene (**2**), 2,7-diiodonaphthalene (**3**), 2,6-diiodonaphthalene (**4**), 1,5-diiodonaphthalene (**5**), 1,6-diiodonaphthalene (**6**), and 1,7-diiodonaphthalene (**7**) were studied in this work.

The preparation of 1,5-diiodonaphthalene and 1,8-diiodonaphthalene followed the procedures reported previously.<sup>2,3</sup> The



preparation of other derivatives was achieved according to the new procedures which are summarized in the Schemes 1 and 2.

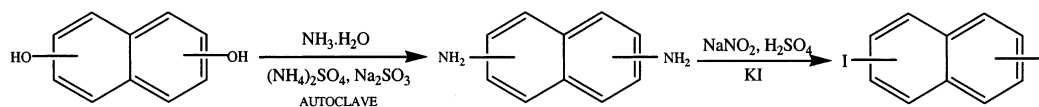
All of the prepared samples were characterized by IR, NMR, elemental analysis, and melting point determinations.

The HeI/HeII photoelectron spectra of the title compounds were recorded on Vacuum Generators UV-G3 spectrometer and calibrated with small amounts of Xe gas which was added to the sample flow. The spectral resolutions in HeI and HeII spectra were 25 and 70 meV, respectively, measured as fwhm of  $^2P_{3/2}$  Ar<sup>+</sup> line. For compounds **1**–**7**, elevated sample temperatures of 140, 120, 150, 150, 160, 150, and 140 °C, respectively, were required in order to achieve sufficient vapor pressures in the sample flow. The spectral bands (for the purposes of relative intensity measurements) were, when necessary, simulated by Gaussian profiles, and baseline corrections were employed (Table 1). The empirical relative intensity, RI (empir) for *i*th band was calculated as

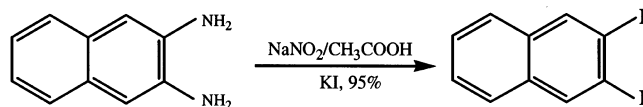
$$RI_i = \{B_i^{\text{HeII}} \cdot \sum_i B_i^{\text{HeI}}\} / \{B_i^{\text{HeI}} \cdot \sum_i B_i^{\text{HeII}}\}$$

where  $B_i$  stands for the band intensity of *i*th band in HeI or HeII spectrum and the index of summation runs through the bands of interest.

## SCHEME 1: 1,6-; 2,6-; 2,7-Diiodonaphthalene



## SCHEME 2: 2,3-Diiodonaphthalene



**Calculations.** All of the calculations were performed with Gaussian 98 program.<sup>4</sup> The DFT calculations with the hybrid B3PW91 functional and the TZP basis set were performed first in order to get fully optimized molecular geometry. Subsequently, single-point ROVGF calculations at B3PW91 geometry were performed in order to obtain ionization energies. The ROVGF method goes beyond Koopmans' approximation and is often used for the assignment of photoelectron spectra.<sup>5</sup>

## Results and Discussion

**Photoelectron Spectra.** The photoelectron spectra are shown in Figures 1-4, and their analysis is summarized in Figure 5 and Table 1. The spectra indicate that the density of ionic states is large, and the information obtained from several empirical and theoretical considerations must be used simultaneously if one is to arrive at a reliable assignment.

The assignments are based on the following considerations. The interpretation of the spectra of diiodonaphthalenes (Figures 1-3) relies on the comparison with the HeI spectrum of naphthalene<sup>6</sup> and HeI/HeII spectra of 1-iodonaphthalene (Figure 4). The spectral region 8–13 eV contains, besides ionizations from five ring  $\pi$ -orbitals ( $\pi$ ), the two out-of-plane iodine lone pairs ( $\pi_I$ ) and two in-plane iodine lone pairs ( $\sigma_I$ ). The relative intensity of bands corresponding to ionizations from the orbitals with large I5p character decreases most prominently on going from HeI to HeII radiation. This is due to different energy dependence of the photoionization cross-sections for I5p and C2p orbitals.<sup>7</sup> The iodine 5p cross-section decreases three times as much as C2p on going from HeI to HeII. The iodine  $\sigma_I$  orbitals can acquire C2p character only by weak interaction with the energetically remote ring  $\sigma$  orbitals (thus  $\sigma_I$  orbitals are prone to show a strong drop in the relative HeII band intensity). The iodine  $\pi_I$  orbitals can, on the other hand, interact strongly with energetically close ring  $\pi$  orbitals and thus acquire C2p character (leading to a modest drop in relative HeII band intensity). The sharp, narrow bands correspond to strongly localized (less bonding) orbitals as is suggested by the Franck–Condon principle.

The assignment of naphthalene spectrum is well established and can be used to analyze the 1-iodonaphthalene spectrum. In the latter's spectrum (Figure 4), the bands at 9.29 and 9.74 eV show a pronounced decrease in relative intensity on going from HeI to HeII radiation. Thus, the two bands can be assigned to ionizations from the two iodine lone pairs; the 9.29 eV band is broader and can be attributed to the out-of-plane lone pair  $\pi_I$  orbital, whereas the 9.74 eV band is narrower which means that the ionized orbital has less bonding character and can thus be described as  $\sigma_I$  orbital. The five ring localized  $\pi$  orbitals can then be attributed to different bands on the basis of comparison with UPS of naphthalene (Figure 5). The assigned spectrum of 1-iodonaphthalene can be utilized as the starting point for the assignment of the spectra of diiodonaphthalenes.

**TABLE 1: Vertical Ionization Energies ( $E_i \pm 0.03$  eV), Calculated Orbital Energies (GF/eV), Band Assignments, and HeI/HeII Relative Band Intensity Ratios (RI) for Orbitals in Iodonaphthalenes<sup>a,b</sup>**

compound	band	$E_i$	GF/eV	MO assignment	RI	
1 ( $C_{2v}$ )	X	(8.00)	7.62	$a_2 (\pi)$	1.96	
	A	8.53	8.18	$b_2 (\sigma_I)$	0.66	
	B	9.13	8.86	$b_1 (\pi)$	1.30	
	C	9.38	8.93	$b_1 (\pi_I)$	1.30	
	D	9.78	9.52	$a_2 (\pi_I)$	0.76	
	E	10.38	10.08	$a_1 (\sigma_I)$	0.61	
	F	10.83	10.81	$b_1 (\pi)$	0.93	
	G	11.15	11.04	$a_1 (\sigma)$	0.93	
	H	11.58	11.69	$a_2 (\pi)$	0.93	
	I	11.95	11.88	$b_2 (\sigma)$	0.93	
	2 ( $C_{2v}$ )	X	(8.14)	7.90	$a_2 (\pi)$	1.10
A		8.58	8.25	$b_1 (\pi)$	1.10	
B		9.17	8.77	$b_2 (\sigma_I)$	0.52	
C		9.70	9.43	$a_2 (\pi_I)$	0.55	
D		10.08	9.79	$b_1 (\pi)$	0.9	
E		10.27	9.90	$a_1 (\sigma_I)$	0.9	
F		10.63	10.48	$a_2 (\pi_I)$	0.75	
G		11.25	11.32	$b_2 (\sigma)$	1.25	
H, I		11.73	11.74, 11.88	$a_1 (\sigma_I), b_1 (\pi)$	1.11	
X		(8.21)	8.01	$a_2 (\pi)$	1.48	
3 ( $C_{2v}$ )		A	8.62	8.26	$b_1 (\pi)$	1.48
	B	9.47	9.38	$b_2 (\sigma_I)$	0.68	
	C	9.70	9.42	$a_2 (\pi_I)$	0.58	
	D, E	9.97	9.42, 9.88	$a_1 (\sigma_I), b_1 (\pi_I)$	0.58	
	F	10.70	10.58	$b_1 (\pi)$	1.17	
	G	11.23	11.31	$b_2 (\sigma)$	1.16	
	H, I	11.80	11.72, 11.96	$a_1 (\sigma), a_2 (\pi)$	1.16	
	X	(8.11)	7.88	$a_u (\pi)$	1.14	
	A	8.77	8.54	$a_u (\pi)$	1.51	
	B	9.31	9.10	$b_g (\pi_I)$	0.50	
	4 ( $C_{2h}$ )	C	9.70	9.40	$b_u (\sigma_I)$	0.36
D		9.92	9.42	$a_g (\sigma_I)$	0.36	
E, F		10.5	10.18, 10.45	$a_u (\pi_I), b_g (\pi)$	1.18	
G		11.27 (11.15)	11.28	$a_g (\sigma)$	1.58	
H, I		11.95	11.97, 11.97	$b_u (\sigma), b_g (\pi)$	1.26	
X		(8.13)	7.85	$a_u (\pi)$	1.23	
A, B		9.08	8.78, 8.92	$a_u (\pi), b_g (\pi_I)$	1.07	
C, D		9.73	9.28, 9.42	$a_g (\sigma_I), b_u (\sigma_I)$	0.56	
E		10.33	9.77	$a_u (\pi_I)$	0.62	
F		10.78	10.80	$b_g (\pi)$	0.97	
G		11.2	11.06	$a_g (\sigma)$	1.40	
5 ( $C_{2h}$ )	H	11.66	11.75	$b_g (\pi)$	1.40	
	I	12.08	12.11	$b_u (\sigma)$	1.40	
	X	(8.12)	7.90	$a'' (\pi)$	1.25	
	A	8.77	8.52	$a'' (\pi)$	1.17	
	B	9.32	9.16	$a'' (\pi_I)$	0.57	
	C	9.65	9.34	$a' (\sigma_I)$	0.57	
	D	9.92	9.42	$a' (\sigma_I)$	0.57	
	E	10.27	9.88	$a'' (\pi_I)$	0.73	
	F	10.70	10.68	$a'' (\pi)$	1.33	
	G	11.27	11.29	$a' (\sigma)$	1.28	
	H, I	11.72	11.68, 11.87	$a' (\sigma), a'' (\pi)$	1.36	
6 ( $C_s$ )	X	(8.07)	7.87	$a'' (\pi)$	1.30	
	A	8.75	8.52	$a'' (\pi)$	0.96	
	B	9.35	9.20	$a'' (\pi_I)$	0.59	
	C	9.60	9.35	$a' (\sigma_I)$	0.59	
	D	9.84	9.36	$a' (\sigma_I)$	0.59	
	E	10.17	9.75	$a'' (\pi_I)$	0.59	
	F	10.77	10.73	$a'' (\pi)$	1.61	
	G	11.27	11.29	$a' (\sigma)$	1.31	
	H, I	11.67	11.64, 11.84	$a' (\sigma), a'' (\pi)$	1.31	
	7 ( $C_s$ )	X	(8.07)	7.87	$a'' (\pi)$	1.30
		A	8.75	8.52	$a'' (\pi)$	0.96
B		9.35	9.20	$a'' (\pi_I)$	0.59	
C		9.60	9.35	$a' (\sigma_I)$	0.59	
D		9.84	9.36	$a' (\sigma_I)$	0.59	
E		10.17	9.75	$a'' (\pi_I)$	0.59	
F		10.77	10.73	$a'' (\pi)$	1.61	
G		11.27	11.29	$a' (\sigma)$	1.31	
H, I		11.67	11.64, 11.84	$a' (\sigma), a'' (\pi)$	1.31	

<sup>a</sup> The values in brackets correspond to adiabatic ionization energies.

<sup>b</sup> The bands were simulated by asymmetric Gaussian band shapes as suggested in ref 13, and the variable bandwidths were in the range 0.1–0.3 eV.

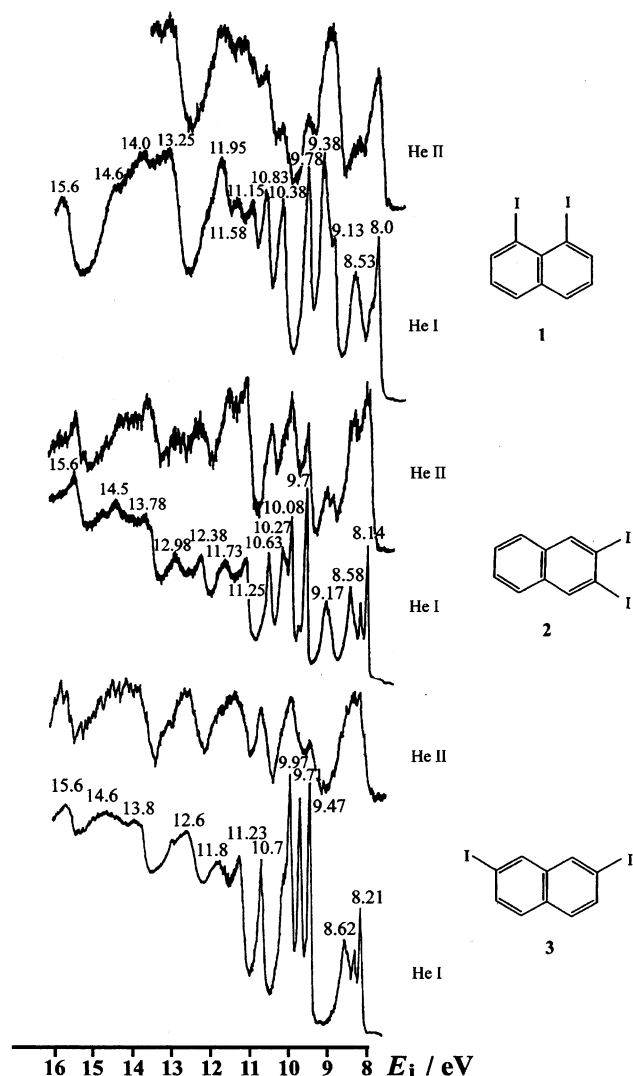
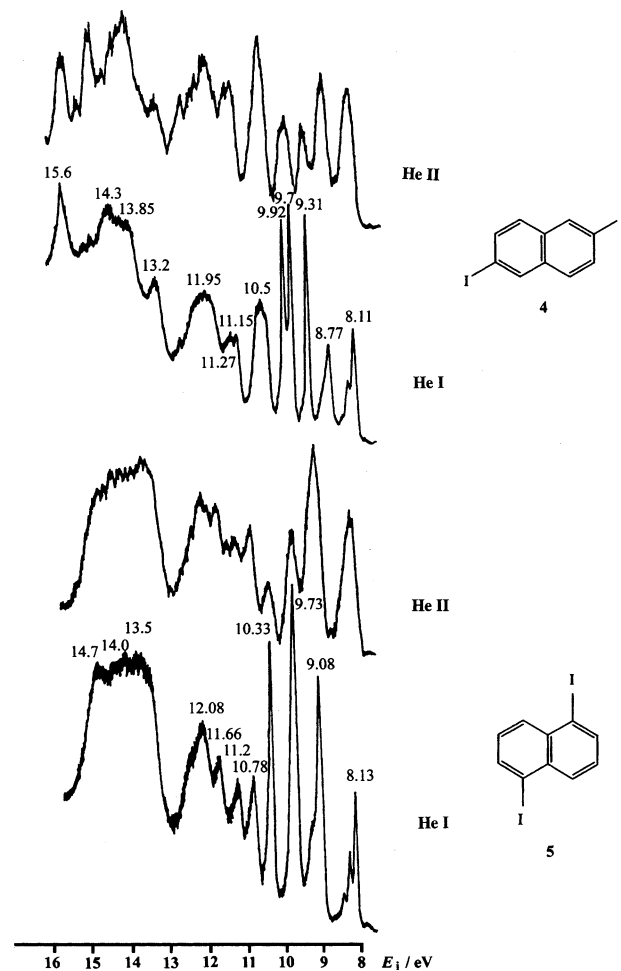


**Figure 1.** HeI/HeII photoelectron spectra of 1–3.

The assignment of the spectrum of **1** (Figure 1) is based on the consideration of relative band intensities in HeI spectrum and HeI/HeII intensity variations. Bands at 8.53, 9.38, 9.78, and 10.38 eV exhibit HeII/HeI intensity decrease and can be attributed to four iodine lone pair ionizations (N.B. 9.38 eV band and the shoulder at 9.13 eV bands comprise two ionizations). The remaining bands can then be attributed to five ring  $\pi$  orbitals and various  $\sigma$  orbitals on the basis of comparison with naphthalene spectrum and GF calculations (Table 1 and Figure 5).

The assignment of the spectra of the remaining diidonaphthalenes **2–7** is based on the same principles as **1**, and we therefore give only the final assignments in Table 1 and Figure 5.

**Intramolecular Interactions.** The most interesting information contained in the UPS data provides insight into the through-bond (TB) and through-space (TS) intramolecular interactions involving I5p orbitals. The total energy range of the I5p manifold ( $\Delta n_I$ ) can be measured directly from the UPS spectra and serves as an internal probe for the total, i.e., TS + TB interactions. However, to fully understand the meaning of numerical values for diidonaphthalenes, we compare their spectra with UPS spectra of diiodobenzenes,<sup>8</sup> diiodoalkanes,<sup>9</sup> and diiodoethenes.<sup>10</sup> The analysis presented in Table 2 suggests the conclusions discussed below.

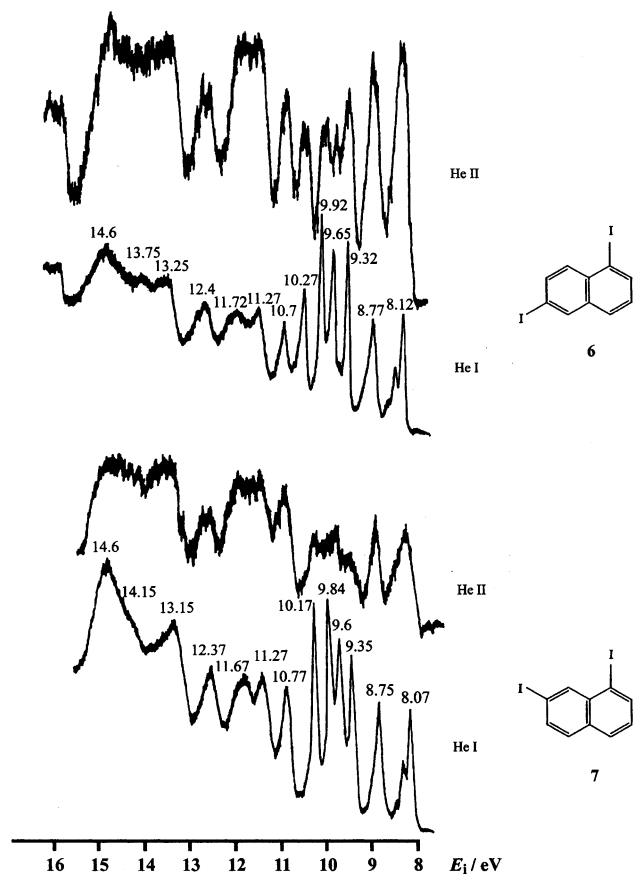


**Figure 2.** HeI/HeII photoelectron spectra of **4** and **5**.

The alkane skeleton is much less efficient than either ethene or aromatic systems in propagating I5p–I5p interactions. This is obvious when one compares small numerical values of  $\Delta n_I$  in diiodoalkanes vs diiodoethenes, diiodobenzenes, and diidonaphthalenes. The reason is in the delocalized nature of  $\pi$  electrons, which are good conduits for such interactions.

The iodine lone pair interactions are larger in diiodobenzenes and diiodoethenes than in diidonaphthalenes (with a single significant exception). This can be attributed to the larger number of intervening CC bonds in diidonaphthalenes. This suggestion is supported by the observation that in **2** the  $\Delta n_I$  is the largest of all isomers except **1**.

In addition to the number of CC bonds, topology of substitution will also influence the magnitude of iodine lone pair interactions. Thus,  $\Delta n_I$  values do not necessarily decrease with the increasing number of bonds separating iodine centers. For example, in **4**, the interaction is larger than in **6** or **7**, even though in **4** there are five intervening CC bonds compared to three or four in the latter molecules. The last important factor which governs iodine lone pair interactions is steric repulsion as is evident from the UPS of *cis* and *trans* 1,2-diiodoethenes, 1,2-diiodobenzene, and 1,8-diidonaphthalene. The iodine lone pair splitting ( $\Delta n_I$ ) in the *cis* isomer is 0.1 eV larger than in the *trans*. The splitting in 1,2-diiodobenzene is smaller (1.73 eV) than in **1** (1.85 eV) despite the general decrease of I5p–I5p interactions on going from diiodobenzenes to diidonaphthalenes (see above). Further evidence in support of this argument comes from the spectrum of **2**. The interaction in **2** is 1.46 eV, which although smaller than in **1** (1.85 eV) is larger

Figure 3. HeI/HeII photoelectron spectra of **6** and **7**.TABLE 2: Energy Range of I5p Manifolds in Iodo-substituted Hydrocarbons ( $\Delta n_I$ /eV)

molecule	$\Delta n_I$	molecule	$\Delta n_I$
ICH <sub>2</sub> I	1.1	1-C <sub>10</sub> H <sub>7</sub> I	0.45
ICH <sub>2</sub> CH <sub>2</sub> I	0.76	1,8-C <sub>10</sub> H <sub>6</sub> I <sub>2</sub>	1.85
ICH <sub>2</sub> CH <sub>2</sub> CH <sub>2</sub> I	0.84	1,5-C <sub>10</sub> H <sub>6</sub> I <sub>2</sub>	1.25
ICH <sub>2</sub> CH <sub>2</sub> CH <sub>2</sub> CH <sub>2</sub> I	0.61	2,3-C <sub>10</sub> H <sub>6</sub> I <sub>2</sub>	1.46
<i>cis</i> -C <sub>2</sub> H <sub>2</sub> I <sub>2</sub>	1.61	2,7-C <sub>10</sub> H <sub>6</sub> I <sub>2</sub>	0.50
<i>trans</i> -C <sub>2</sub> H <sub>2</sub> I <sub>2</sub>	1.53	2,6-C <sub>10</sub> H <sub>6</sub> I <sub>2</sub>	1.19
1,2-C <sub>6</sub> H <sub>4</sub> I <sub>2</sub>	1.73	1,6-C <sub>10</sub> H <sub>6</sub> I <sub>2</sub>	0.95
1,3-C <sub>6</sub> H <sub>4</sub> I <sub>2</sub>	1.20	1,7-C <sub>10</sub> H <sub>6</sub> I <sub>2</sub>	0.82
1,4-C <sub>6</sub> H <sub>4</sub> I <sub>2</sub>	1.54		

than in **5** (1.25 eV). This is due to spatial distances between respective iodine atoms in the three molecules. The iodine atom positions in **5** preclude steric repulsion and TS interaction. In **2**, the I–I distance is larger (3.64 Å)<sup>11</sup> than in **1** (3.53 Å)<sup>1</sup> which is reflected in the respective  $\Delta n_I$  values. It is possible to estimate contributions to measured energy splitting arising from through-space interactions. Comparing values in **1** and **5**, the TS interaction value is 0.6 eV. Comparing UPS data for **1** and **2** gives a TS difference of 0.21 eV. It is also possible to deduce TS contribution in diiodobenzenes by comparing 1,2- with 1,4-diiodobenzene, which gives the TS contribution of 0.19 eV. It can then be tentatively suggested that the TS interactions in **1** are approximately three times larger than in either 1,2-diiodobenzene or **2**.

It is interesting to compare the steric repulsion in diionaphthalenes with their bis-methylamino substituted analogues. UPS has revealed that the nitrogen lone pair interactions increase from 0.82 to 2.0 eV on going from 1,5-bis(dimethylamino)naphthalene to its 1,8-isomer.<sup>12</sup> This increase of 1.18 eV is twice as large as the 0.6 eV in diiodonaphthalene counterparts. Although the nitrogen atom is smaller than iodine, the presence

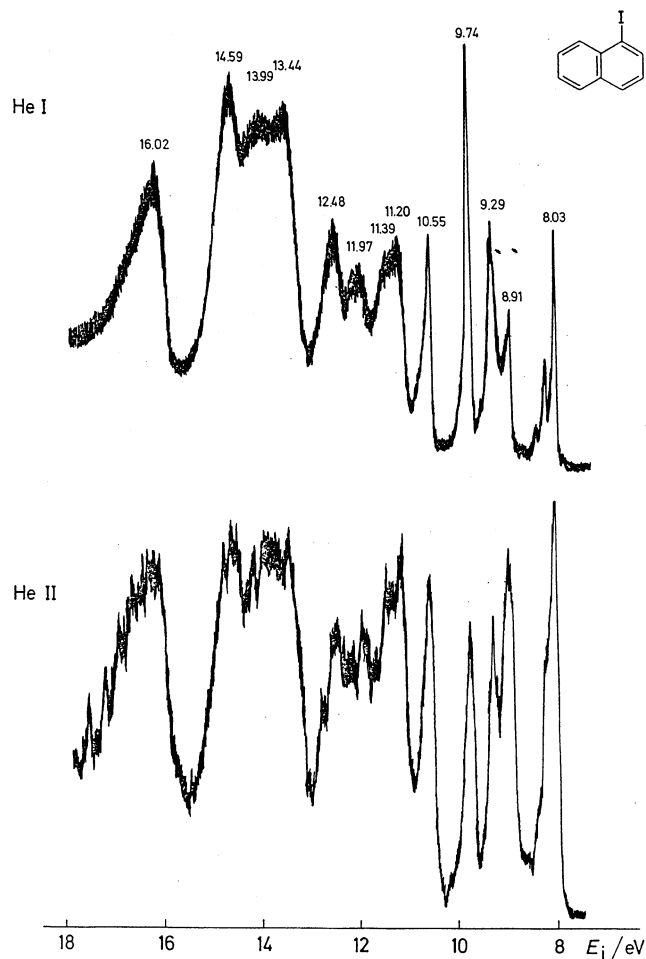


Figure 4. HeI/HeII photoelectron spectra of 1-iodonaphthalene.

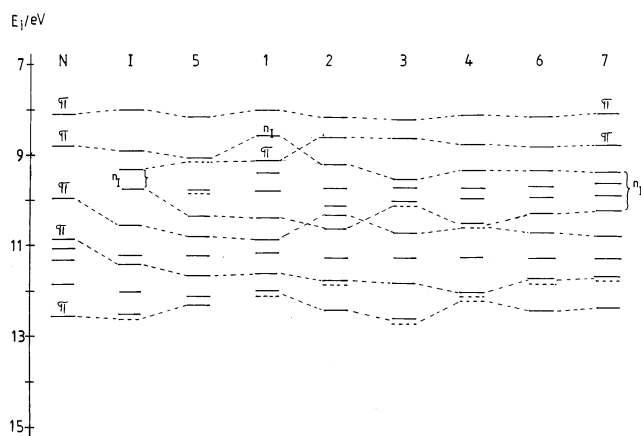


Figure 5. Energy level diagram for diiodonaphthalenes.

of more strongly localized electron lone pairs in the former may account for the difference in steric repulsion.

## Conclusion

The analysis of UPS data for diiodonaphthalenes provides interesting semiquantitative insights into the nature of steric repulsions and TS interactions. The 1,8-diiodonaphthalene is a prime example of strong steric interactions. The single reported X-ray study<sup>1</sup> suggested that such interactions are prominent. However, because of the complexities associated with crystal packing forces, the observed crystal structure could not provide a clear answer regarding the extent of molecular distortion. The UPS data collected in the gas phase are free from such

complications and do not depend on approximations inherent in theoretical models describing steric interactions. Nonetheless, it would be interesting if the results of the gas-phase electron diffraction study were to become available in the future to complement our UPS study. In that case, the molecular distortion and TS interactions could be related directly.

**Supporting Information Available:** Geometries and computed total energies. This material is available free of charge via the Internet at <http://pubs.acs.org>.

## References and Notes

- (1) Bock, H.; Sievert, M.; Havlas, Z. *Chem. Eur. J.* **1998**, *4*, 677.
- (2) Hodgson, H. H.; Whitehurst, J. S. *J. Chem. Soc.* **1947**, 80.
- (3) House, H. O.; Koepsell, D. G.; Campbell, W. J. *J. Org. Chem.* **1972**, *37*, 1003.
- (4) Frisch, M. J.; Trucks, G. W.; Schlegel, H. B.; Scuseria, G. E.; Robb, M. A.; Cheeseman, J. R.; Zakrzewski, V. G.; Montgomery, J. A., Jr.; Stratmann, R. E.; Burant, J. C.; Dapprich, S.; Millam, J. M.; Daniels, A. D.; Kudin, K. N.; Strain, M. C.; Farkas, O.; Tomasi, J.; Barone, V.; Cossi, M.; Cammi, R.; Mennucci, B.; Pomelli, C.; Adamo, C.; Clifford, S.; Ochterski, J.; Petersson, G. A.; Ayala, P. Y.; Cui, Q.; Morokuma, K.; Malick, D. K.; Rabuck, A. D.; Raghavachari, K.; Foresman, J. B.; Cioslowski, J.; Ortiz, J. V.; Stefanov, B. B.; Liu, G.; Liashenko, A.; Piskorz, P.; Komaromi, I.; Gomperts, R.; Martin, R. L.; Fox, D. J.; Keith, T.; Al-Laham, M. A.; Peng, C. Y.; Nanayakkara, A.; Gonzalez, C.; Challacombe, M.; Gill, P. M. W.; Johnson, B. G.; Chen, W.; Wong, M. W.; Andres, J. L.; Head-Gordon, M.; Replogle, E. S.; Pople, J. A. *Gaussian 98*, revision A.11; Gaussian, Inc.: Pittsburgh, PA, 1998.
- (5) Potts, A. W.; Trofimov, A. B.; Schirmer, J.; Holland, D. M. P.; Karlsson, L. *Chem. Phys.* **2001**, *271*, 337.
- (6) Klasinc, L.; Kovač, B.; Güsten, H. *Pure Appl. Chem.* **1983**, *55*, 289.
- (7) Yeh, J. J. *Atomic Calculation of Photoionization Cross-sections and Asymmetry Parameters*; Gordon and Breach: Langhorne 1993.
- (8) Cvitaš, T.; Güsten, H.; Klasinc, L. *J. Chem. Soc. Perkin Trans. 2* **1977**, 962.
- (9) Novak, I.; Klasinc, L.; Kovač, B.; McGlynn, S. P. *J. Mol. Struct.* **1993**, *297*, 383.
- (10) Wittel, K.; Bock, H.; Manne, R. *Tetrahedron* **1974**, *30*, 651.
- (11) Huiming, J.; Novak, I. Unpublished X-ray results
- (12) Maier, J. P. *Helv. Chim. Acta* **1974**, *57*, 994.
- (13) Lichtenberger, D. L.; Copenhaver, A. S. *J. Electron Spectrosc. Relat. Phenom.* **1990**, *50*, 335.